


SHORT COMMUNICATION

Antiferromagnetism and p-type conductivity of nonstoichiometric nickel oxide thin films

Mari Napari¹  | Tahmida N. Huq¹ | Tuhin Maity¹ | Daisy Gomersall² | Kham M. Niang² | Armin Barthel¹ | Juliet E. Thompson¹ | Sami Kinnunen³ | Kai Arstila³ | Timo Sajavaara³ | Robert L. Z. Hoye¹ | Andrew J. Flewitt² | Judith L. MacManus-Driscoll¹

¹Department of Materials Science and Metallurgy, University of Cambridge, Cambridge, UK

²Electrical Engineering Division, Department of Engineering, University of Cambridge, Cambridge, UK

³Department of Physics, University of Jyväskylä, Jyväskylä, Finland

Correspondence

Mari Napari, Department of Materials Science and Metallurgy, University of Cambridge, Cambridge, UK.

Email: m.p.napari@soton.ac.uk

Present address

Mari Napari, Zepler Institute for Photonics and Nanoelectronics, University of Southampton, Southampton, UK.

Funding information

Aziz Foundation; Engineering and Physical Sciences Research Council, Grant/Award Numbers: EP/L0160871, EP/P027032/1; European Commission, Grant/Award Number: H2020-MSCA-IF-2016 745886 MuStMAM; Isaac Newton Trust, Grant/Award Number: RG96474; Royal Academy of Engineering, Grant/Award Number: RF/201718/17101

KEYWORDS: atomic layer deposition, chemical vapor deposition, nickel oxide, solution deposition, thin films

Nickel oxide (NiO) is one of the most studied transition metal oxides due to its versatile chemical and electronic properties, enabling it to be used in a wide variety of applications. In its stoichiometric form, NiO is an antiferromagnetic insulator, with resistivity up to $10^{13} \Omega \text{ cm}$.¹ When Ni vacancies are introduced, the nonstoichiometric nickel oxide becomes a semiconductor. Both theoretical and experimental results have shown that in oxygen-rich conditions the formation energy of the Ni vacancies is the lowest for all defects, leading to p-type conduction.^{2,3} With a wide band gap (3.5–4.0 eV) and high work function (4.8–6.7 eV), depending on the crystalline structure, composition, and the processing of the films,^{4,5} nickel oxide has gained interest especially in optoelectronics,

where it is used as a hole transport/injection layer for photovoltaics and light-emitting diodes.^{6,7} Nickel oxide thin films have also been shown to have great potential across a wide range of electronics applications from gas sensors to thin film transistors and resistive switching random access memory (ReRAM) devices.^{8–10} These include flexible electronic devices, in which nickel oxide has been shown to be stable after exposure to tensile or compressive strains.^{11,12} Many of these applications rely on nickel oxide being nonstoichiometric, which has a significant effect on the electrical properties. The antiferromagnetic nature of the NiO has made it a common material in spintronics research,¹³ for example, in the fabrication of spin valves¹⁴ and next-generation memory

This is an open access article under the terms of the Creative Commons Attribution License, which permits use, distribution and reproduction in any medium, provided the original work is properly cited.

© 2020 The Authors. *InfoMat* published by John Wiley & Sons Australia, Ltd on behalf of UESTC.

technologies.¹⁵ In all of these applications, a well-controlled growth process of the materials is required. Physical vapor deposition techniques, such as pulsed laser deposition and sputtering, can provide excellent control over film stoichiometry^{16,17} but can be incompatible with some applications and device integration.

Chemical routes, including chemical vapor deposition techniques and solution processing, can provide a straightforward way to coat large areas uniformly at low temperatures, but the growth is governed by the chemistry, with little control over the film composition and properties.

In this work, NiO thin films were grown using plasma-enhanced atomic layer deposition (PEALD), and the composition together with the optical, electrical, and magnetic properties were characterized. The magnetic properties of ALD-grown nickel oxide films have been reported before, for example, by Bachmann et al¹⁸ indicating room-temperature diamagnetism, but the results were inconclusive. Additionally, we compare the PEALD nickel oxide to the films deposited with other chemical deposition techniques, that is, atmospheric pressure chemical vapor deposition and solution processing for better understanding of the significance of the deposition method on the microstructure, stoichiometry, and consequently, the electrical and magnetic properties (see Supporting Information).

Nickel oxide films were deposited at 200°C on Si, SiO₂/Si, and borosilicate glass substrates using PEALD with nickel(II) acetylacetonate (Ni(acac)₂) and direct oxygen plasma. Ni(acac)₂ was chosen as the Ni precursor because it is widely available and inexpensive. Ni(acac)₂ does not pose any significant risk to the user or the environment, and has a low reactivity at ambient conditions, which makes it easy to handle. Ni(acac)₂ has a low reactivity toward water, but it has been successfully demonstrated in thermal ALD growth of nickel oxide with ozone at temperatures of 175 to 300°C,^{19,20} with the lower temperature limit defined by the vapor pressure of the Ni(acac)₂. However, the use of ozone is not ideal for large-area deposition as nickel oxide is known to be a highly effective catalyst for ozone decomposition.²¹ The use of direct O₂ plasma also increases the process efficiency, as it enables the use of short plasma pulses. Here, 4 seconds pulses were enough for saturated growth, while in reports of PEALD nickel oxide with remote plasma, pulses of 15 to 30 seconds are required to achieve saturation and uniform growth under moderate vacuum conditions.^{22,23}

Two film thicknesses, 50 and 170 nm, were grown for different measurements. X-ray diffraction measurements indicated that the films were polycrystalline cubic NiO with clear (200) preferred orientation (Figure 1) and

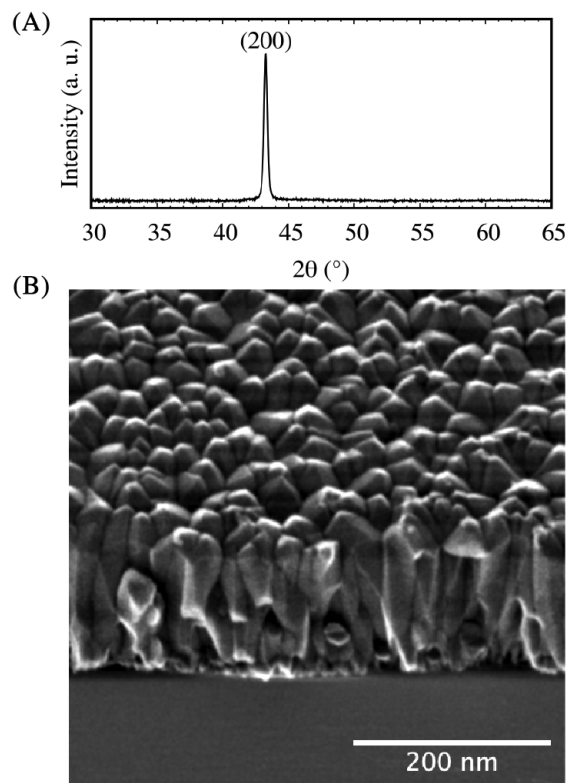


FIGURE 1 A, XRD pattern of the PEALD grown 170 nm nickel oxide film showing dominant (200) orientation. B, a HIM cross-section image of the corresponding PEALD nickel oxide film on Si, sample tilt is 40°. PEALD, plasma-enhanced atomic layer deposition

crystallite size of ca. 35 nm, calculated using the Scherrer equation. The lattice constant of $a = 0.4185 \text{ \AA}$ is slightly higher than the literature value for the bulk NiO at room temperature (0.4176 \AA), affected by the film non-stoichiometry or the residual stress in the films. A film density of 6.2 g cm^{-3} was determined using X-ray reflectometry. The film RMS roughness, measured with atomic force microscopy, was ca. 2 nm for the 50 nm thick films (Figure S3). Further investigation of the film microstructure with cross-sectional imaging of the thicker films using helium ion microscopy showed that the films initially grow from the substrate with a random orientation for a few tens of nanometers, after which the grains have (200) preferred orientation, forming large column-like structures (Figure 1).

The film composition was determined using both X-ray photoelectron spectroscopy (XPS) and time-of-flight elastic recoil detection analysis (ToF-ERDA). ToF-ERDA depth profiling (Figure 2) showed that the films were non-stoichiometric with significant nickel deficiency, Ni = 40 at.%, O = 57 at.%, corresponding to Ni/O = 0.7. Apart from nickel and oxygen, the films contain a small amount of light element impurities, that is, ~3 at.-% hydrogen, 0.3 at.-% carbon, and 0.5 at.-% nitrogen

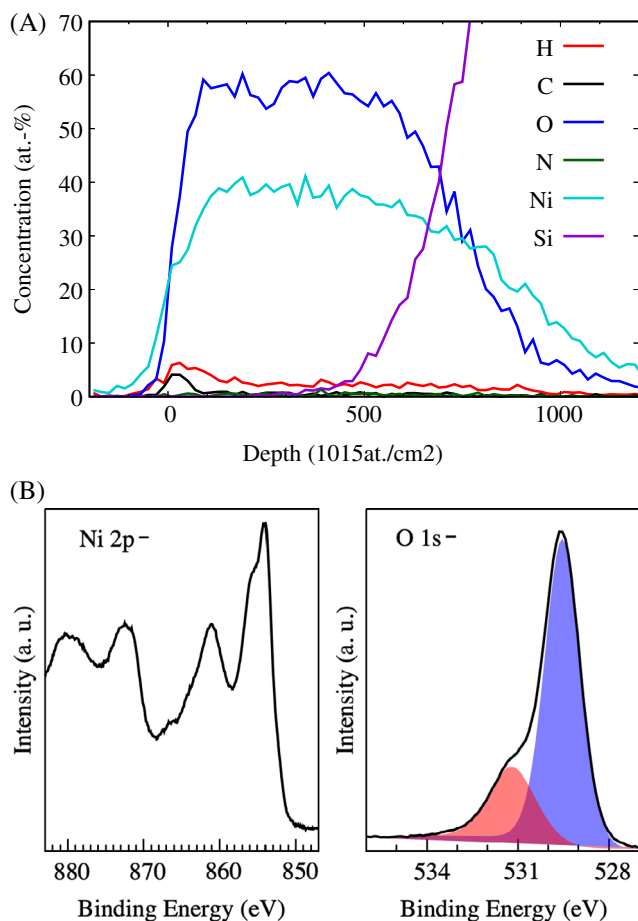


FIGURE 2 A, ToF-ERDA depth profile of a 50 nm PEALD nickel oxide film. B, XPS spectra of Ni 2p and O 1s electrons of a corresponding film. The blue and red peak in the O 1s spectrum refer to NiO lattice oxygen and defective sites, respectively. PEALD, plasma-enhanced atomic layer deposition; ToF-ERDA, time-of-flight elastic recoil detection analysis

(see Table S1 of supporting information). Of these H, C originate from the Ni(acac)₂ precursor while nitrogen is incorporated into the films during the pulsing of the O₂/N₂ plasma gas mixture. The impurity contents are also significantly lower than in films deposited with other chemical methods (see Table S1). The low impurity content also confirmed the suitability of the PEALD method with Ni(acac)₂ precursor for the growth of nickel oxide films, as PEALD processes for β -diketonate precursors for growth of nickel oxide films have not been reported before,²²⁻²⁴ and the thermal ALD processes can suffer from high concentrations of carbon impurities.²⁵ XPS results, shown in Figure 2 are in accordance with the ToF-ERDA, showing a nonstoichiometric composition (see Table S1). The spectrum of O 1s binding energy indicates defective oxide content in the films, seen as the peak at 531.4 eV, typically associated with the presence of Ni³⁺ and corresponding Ni vacancies. Similar features in the O 1s spectrum have also been associated with hydroxide

(-OH) species, but the low H content measured with ToF-ERDA does not support this assumption. However, the quantitative determination of the amount of nickel vacancies in the films, that is, Ni²⁺/Ni³⁺ ratio, from the XPS spectra is challenging due to the complexity of the Ni 2p peak shapes resulting from multiplet splitting, shake-up, and plasmon loss structure.²⁶

The electrical properties of the films were characterized by Hall effect measurement. The resistivity of 50 nm films was 80 Ω cm, measured using a van der Pauw configuration, which is in accordance with the film composition corresponding with an increase in the free-hole concentration by the Ni vacancy ionization. The resistivity of 170 nm films was ca. 200 Ω cm. The films were confirmed to have p-type conductivity, with a hole density of $\sim 10^{17}$ cm⁻³ and mobility ~ 0.1 cm² V⁻¹ s⁻¹, independent of the film thickness. However, antiferromagnetic behavior of the films (see discussion next) could add significant uncertainty to the Hall effect measurements. The resistivity values are consistent with what has been reported for ALD- and CVD-grown nickel oxide.²⁷⁻²⁹ The mobility and carrier density values are in accordance with what has been reported from Hall measurements of vapor deposited nickel oxide thin films,²⁸ but vary by a few orders of magnitude from what has been derived from electrochemical impedance spectroscopy data.^{6,29,30} In addition, a thermal activation energy (E_a) of 0.31 eV was determined using a two-point-probe measurement within a temperature range of 25°C to 130°C and the Arrhenius relation (Figure S7). The E_a indicates the position of the Fermi level from the valence band edge. The obtained E_a is consistent with values extracted from nickel oxide thin films with similar resistivity grown by other chemical methods.^{31,32}

The magnetic properties of the films were investigated using a magnetometer with ± 70 kOe field and 1.8 to 400 K temperature range. The hysteresis loops for the 50 nm nickel oxide film, measured at 2 K temperature, show linear behavior (Figure 3) with nearly zero coercivity (H_c) and remanence (M_R). The magnetization does not saturate within the field range of ± 70 kOe. The temperature-dependent magnetization curve shows no bi-furcation between the zero-field cooled (ZFC) and 100 Oe field cooled (FC) curve. No remanence magnetization (M_R) was observed within the measured temperature range (350-2 K), as seen in the inset of Figure 3. This indicates a strong antiferromagnetic property of the films throughout the temperature range.

To further confirm the antiferromagnetism of the nonstoichiometric nickel oxide thin films, the exchange bias (EB) effect was investigated in-plane. For this, 6 nm of Ni₈₀Fe₂₀ (Py) was deposited on PEALD nickel oxide by DC magnetron sputtering. Since Py is ferromagnetic, an

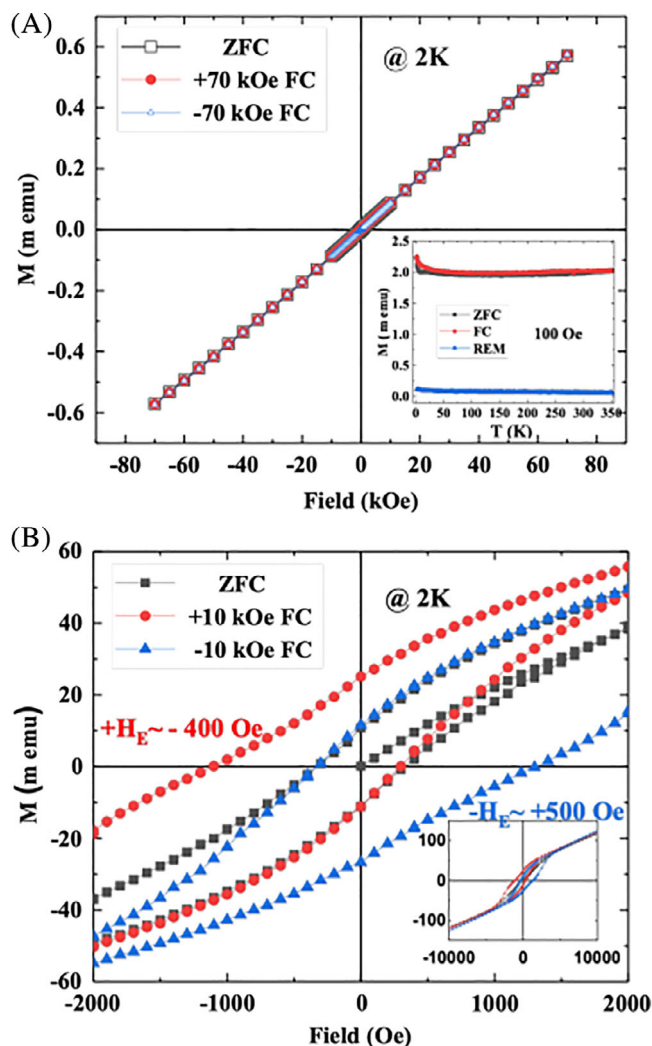


FIGURE 3 A, The hysteresis loops of a bare 50 nm nickel oxide film shows linear behavior and no saturation. The magnetization vs temperature curve (inset) shows no significant change for ZFC and FC measurements. B, Exchange bias ($H_E \approx 400$ –500 Oe) was observed at 2 K in Py (6 nm)/NiO_x(50 nm) bilayer film, FC ± 10 kOe. Inset figure shows the saturation of Py film and unsaturated NiO_x film. FC, field cooled; ZFC, zero-field cooled

EB shift (H_E) should be observed if the nickel oxide film is antiferromagnetic. Figure 3 shows a clear EB behavior measured in the Py (6 nm)/Ni_{1-x}O (50 nm) bilayer film. The initial hysteresis loop (ZFC loop) which starts from (0,0) confirms a complete demagnetization of the film by the applied protocol (see Supporting Information) and that no stray field is present in the superconducting coil of the magnetometer. For ZFC, no H_E was present. For positive 10 kOe (negative -10 kOe) applied bias field, the FC hysteresis loop shifts toward negative (positive) field direction. The magnitude of EB shift for positive bias field is $+H_E \approx -400$ Oe and for negative bias field $-H_E \approx 500$ Oe. Such asymmetry in EB is often observed in

antiferromagnetic oxides.³³ The ferromagnetic Py saturates at a very high field of ≈ 5 kOe and the coercivity is also high ~ 700 to 800 Oe compared with bare Py, as seen in the inset of Figure 3. This is due to the strong EB coupling between the Py and nickel oxide.³⁴

We have shown that a β -diketonate type precursor can be used in an efficient PEALD process to grow nickel oxide thin films. The nonstoichiometric nickel oxide films are highly crystalline and have a dense microstructure, low impurity content, and high nickel vacancy concentration leading to p-type conductivity. The low concentration of hydrogen impurities is important for films used in electrical applications, as it has been shown that in wide band gap oxide hydrogen can act as compensating center that always counteracts the prevailing conductivity.³⁵ In addition to structural and electrical characterization, the magnetic behavior of the films was thoroughly screened. Here, we confirm that the nickel oxide thin films remain antiferromagnetic despite the significant deviation from the NiO stoichiometry. The comparison to other chemical vapor and solution deposition techniques showed that nickel deficient films are grown with these techniques and while the choice of deposition method has an effect on the microstructure and characteristics of the films, the basic properties of the nonstoichiometric nickel oxide, including antiferromagnetism, persist (See Supporting Information). This underlines the potential of ALD and other chemical routes in fabrication of thin films for different device applications requiring p-type conductivity and/or antiferromagnetism.

ACKNOWLEDGMENTS

Mr. Chris Amey is acknowledged for the XPS measurements, and Mr. Jerome Innocent for measuring UVVis of the PEALD and AP-CVD samples. M.N. and J.L. M.-D. acknowledge funding from the EPSRC grant EP/P027032/1. T.N.H. acknowledges funding from the EPSRC Centre for Doctoral Training in Graphene Technology (No. EP/L0160871) and Aziz Foundation. T.M. and J.L.M.-D. acknowledge funding from EU grant H2020-MSCA-IF-2016 745886 MuStMAM and Isaac Newton Trust (RG96474). R.L.Z.H. acknowledges funding from the Royal Academy of Engineering via the Research Fellowship scheme (No.: RF/201718/17101), as well as support from Magdalene College Cambridge.

CONFLICT OF INTEREST

The authors declare that there is no conflict of interest regarding the publication of this article.

ORCID

Mari Napari  <https://orcid.org/0000-0003-2690-8343>

REFERENCES

- Nachman M, Cojocaru LN, Ribco LV. Electrical properties of non-stoichiometric nickel oxide. *Phys Stat Sol.* 1965;8: 773-783.
- Pizzini S, Morlotti R. Thermodynamic and transport properties of stoichiometric and nonstoichiometric nickel oxide. *J Electrochem Soc.* 1967;114(11):1179-1189.
- Dawson JA, Guo Y, Robertson J. Energetics of intrinsic defects in NiO and the consequences for its resistive random access memory performance. *Appl Phys Lett.* 2015;107:122110.
- Greiner MT, Helander MG, Wang ZB, Tang W-M, Lu Z-H. Effects of processing conditions on the work function and energy-level alignment of NiO thin films. *J Phys Chem C.* 2010; 114(46):19777-19781.
- Hietzschold S, Hillebrandt S, Ullrich F, et al. Functionalized nickel oxide hole contact layers: work function versus conductivity. *ACS Appl Mater Inter.* 2017;9(45):39821-39829.
- Zhao B, Lee LC, Yang L, et al. In situ atmospheric deposition of ultrasmooth nickel oxide for efficient perovskite solar cells. *ACS Appl Mater Inter.* 2018;10(49):41849-41854.
- Gangishetty MK, Hou S, Quan Q, Congreve DN. Reducing architecture limitations for efficient blue perovskite light-emitting diodes. *Adv Mater.* 2018;30:1706226.
- Kim H-J, Lee J-H. Highly sensitive and selective gas sensors using p-type oxide semiconductors: overview. *Sensor Actuat B-Chem.* 2014;192:607-627.
- Lee CT, Chen C-C, Lee H-Y. Three dimensional- stacked complementary thin-film transistors using n-type Al:ZnO and p-type NiO thin-film transistors. *Sci Rep.* 2018;8:3968.
- Russo U, Ielmini D, Cagli C, Lacaíta AL. Filament conduction and reset mechanism in NiO-based resistive-switching memory (RRAM) devices. *IEEE T Electron Dev.* 2009;56(2):186-192.
- Münzenrieder N, Zysset C, Petti L, Kinkeldei T, Salvatore GA, Tröster G. Room-temperature fabricated flexible NiO/IGZO pn diode under mechanical strain. *Solid State Electron.* 2013;87: 17-20.
- Wang H, Zou C, Zhou L, Tian C, Fu D, Tröster G. Resistive switching characteristics of thin NiO film based flexible nonvolatile memory devices. *Microelectron Eng.* 2012;91: 144-146.
- Jungfleisch MB, Zhang W, Hoffmann A. Perspectives of antiferromagnetic spintronics. *Phys Lett A.* 2018;382(13):865-871.
- Chopra HD, Yang DX, Chen PJ, Parks DC, Egelhoff WF. Nature of coupling and origin of coercivity in giant magnetoresistance NiO-co-cu-based spin valves. *Phys Rev B.* 2000;61(14): 9642-9652.
- Zelezny J, Wadley P, Olejnik K, Hoffmann A, Ohno H. Spin transport and spin torque in antiferromagnetic devices. *Nat Phys.* 2018;14:220-228.
- Zhang JY, Li WW, Hoye RLZ, et al. Electronic and transport properties of Li-doped NiO epitaxial thin films. *J Mater Chem C.* 2018;6(9):2275-2282.
- Lu YM, Hwang WS, Yang JS, Chuang HC. Properties of nickel oxide thin films deposited by RF reactive magnetron sputtering. *Thin Solid Films.* 2002;420-421:54-61.
- Bachmann J, Zolotaryov A, Albrecht O, et al. Stoichiometry of nickel oxide films prepared by ALD. *Chem Vapor Depos.* 2011; 17:177-180.
- Utriainen M, Kroger-Laukkanen M, Niinistö L. Studies of NiO thin film formation by atomic layer epitaxy. *Mat Sci Eng B.* 1998;54(1-2):98-103.
- Bratvold JE, Fjellvåg H, Nilsen O. Atomic layer deposition of oriented nickel titanate (NiTiO₃). *Appl Surf Sci.* 2014;311: 478-489.
- Stoyanova M, Konova P, Nikolov P, Naydenov A, Christoskova S, Mehandjiev D. Alumina-supported nickel oxide for ozone decomposition and catalytic ozonation of CO and VOCs. *Chem Eng J.* 2006;122(1):41-46.
- Hufnagel AG, Henß A-K, Hoffmann R, et al. Electron-blocking and oxygen evolution catalyst layers by plasma-enhanced atomic layer deposition of nickel oxide. *Adv Mater Interfaces.* 2018;5(16):1701531.
- Koshtyal Y, Nazarov D, Ezhov I, et al. Atomic layer deposition of NiO to produce active material for thin-film lithium-ion batteries. *Coatings.* 2019;9(5):301.
- Holden KEK, Dezelah CL, Conley JF. Atomic layer deposition of transparent p-type semiconducting nickel oxide using Ni(tBu₂DAD)₂ and ozone. *ACS Appl Mater Inter.* 2019;11(33): 30437-30445.
- Lindahl E, Ottosson M, Carlsson J-O. Atomic layer deposition of NiO by the Ni(thd)₂/H₂O precursor combination. *Chem Vapor Depos.* 2009;15(7-9):186-191.
- Biesinger MC, Payne BP, Lau LWM, Gerson A, Smart RSC. X-ray photoelectron spectroscopic chemical state quantification of mixed nickel metal, oxide and hydroxide systems. *Surf Interface Anal.* 2009;41(4):324-332.
- Battiatto S, Giangregorio MM, Catalano MR, Lo Nigro R, Losurdo M, Malandrino G. Morphology controlled synthesis of NiO films: the role of the precursor and the effect of the substrate nature on the films' structural/optical properties. *RSC Adv.* 2016;6(37):30813-30823.
- Wang H, Guoguang W, Cai XP, et al. Effect of growth temperature on structure and optical characters of NiO films fabricated by PA-MOCVD. *Vacuum.* 2012;86(12):2044-2047.
- Koushik D, Jošt M, Dučinskas A, et al. Plasma-assisted atomic layer deposition of nickel oxide as hole transport layer for hybrid perovskite solar cells. *J Mater Chem C.* 2019;7(40): 12532-12543.
- Thimsen E, Martinson ABF, Elam JW, Pellin MJ. Energy levels, electronic properties, and rectification in ultrathin p-NiO films synthesized by atomic layer deposition. *J Phys Chem C.* 2012;116(32):16830-16840.
- Patil PS, Kadam L. Preparation and characterization of spray pyrolyzed nickel oxide (NiO) thin films. *Appl Surf Sci.* 2002;199 (1-4):211-221.
- Soleimanpour AM, Jayatissa AH, Sumanasekera G. Surface and gas sensing properties of nanocrystalline nickel oxide thin films. *Appl Surf Sci.* 2013;276:291-297.
- Maity T, Roy S. Asymmetric shift of exchange bias loop in Ni-Ni(OH)₂ core-shell nanoparticles. *J Magn Magn Mater.* 2018; 465:100-105.
- Luches P, Benedetti S, Bona A, Valeri S. Magnetic couplings and exchange bias in Fe/NiO epitaxial layers. *Phys Rev B.* 2010; 81(5):054431.
- Li H, Robertson J. Behaviour of hydrogen in wide band gap oxides. *J Appl Phys.* 2014;115(20):203708.

SUPPORTING INFORMATION

Additional supporting information may be found online in the Supporting Information section at the end of this article.

How to cite this article: Napari M, Huq TN, Maity T, et al. Antiferromagnetism and p-type conductivity of nonstoichiometric nickel oxide thin films. *InfoMat*. 2020;1–6. <https://doi.org/10.1002/inf2.12076>